

Biosynthesis of Actinorhodin and Related Antibiotics: Discovery of Alternative Routes for Quinone Formation Encoded in the *act* Gene Cluster

Susumu Okamoto,^{1,3} Takaaki Taguchi,^{2,3} Kozo Ochi,^{1,*} and Koji Ichinose^{2,*}

¹National Food Research Institute, Kannondai, Tsukuba 305-8642, Japan

²Research Institute of Pharmaceutical Sciences, Musashino University, Shinmachi, Nishitokyo-shi, Tokyo 202-8585, Japan

³These authors contributed equally to this work.

*Correspondence: kochi@affrc.go.jp (K.O.), ichinose@musashino-u.ac.jp (K.I.)

DOI 10.1016/j.chembiol.2009.01.015

SUMMARY

All known benzoisochromanquinone (BIQ) biosynthetic gene clusters carry a set of genes encoding a two-component monooxygenase homologous to the ActVA-ORF5/ActVB system for actinorhodin biosynthesis in *Streptomyces coelicolor* A3(2). Here, we conducted molecular genetic and biochemical studies of this enzyme system. Inactivation of *actVA-ORF5* yielded a shunt product, actinoperylone (ACPL), apparently derived from 6-deoxy-dihydro-kalafungin. Similarly, deletion of *actVB* resulted in accumulation of ACPL, indicating a critical role for the monooxygenase system in C-6 oxygenation, a biosynthetic step common to all BIQ biosyntheses. Furthermore, *in vitro*, we showed a quinone-forming activity of the ActVA-ORF5/ActVB system in addition to that of a known C-6 monooxygenase, ActVA-ORF6, by using emodinanthrone as a model substrate. Our results demonstrate that the *act* gene cluster encodes two alternative routes for quinone formation by C-6 oxygenation in BIQ biosynthesis.

INTRODUCTION

Bacteria of the genus *Streptomyces* are one of the most important groups of microorganisms in producing a huge variety of secondary metabolites, including antibiotics (Chater and Hopwood, 1993). Actinorhodin (ACT) **1** is a blue-pigmented antibiotic produced by *Streptomyces coelicolor* A3(2), which is genetically the most-characterized actinomycete (Bentley et al., 2002). ACT belongs to a class of aromatic polyketides, the benzoisochromanquinone (BIQ) antibiotics. Historically, ACT **1** is the first antibiotic whose whole biosynthetic gene cluster was cloned and has served as one of the best model compounds for studying type II polyketide synthase (PKS), their ancillary enzymes, and subsequent post-PKS tailoring enzymes. Consequently, numerous studies have provided much important information on ACT biosynthesis. Recent advances in understanding the fundamental processes revealed mechanistic details of the assembly of the basic carbon skeleton accomplished by the type II minimal

PKS (Beltran-Alvarez et al., 2007); conversion of the octaketide to the bicyclic intermediate **2** catalyzed by the ketoreductase (KR) for the C-9 position (Korman et al., 2008); and the stereospecific ketoreduction at C-3, leading to the first chiral biosynthetic intermediate, 4-dihydro-9-hydroxy-1-methyl-10-oxo-3-*H*-naphtho-[2,3-*c*]-pyran-3-(*S*)-acetic acid, (*S*)-DNPA **3** (Itoh et al., 2007). Subsequent oxygenation at the C-6 position (Figure 1A) is the key step to complete BIQ chromophore synthesis, and biochemical (Kendrew et al., 1997) and crystallographic (Sciara et al., 2003) studies showed that the ActVA-ORF6 protein functions as a C-6 monooxygenase, which, unusually, requires no prosthetic group, metal ion, or cofactor. At present, however, there is no *in vivo* evidence for the involvement of ActVA-ORF6 in C-6 oxygenation.

Two other complete biosynthetic gene clusters for the BIQs (Figures 1B and 1C) have been cloned and sequenced to date: granaticin (GRA) **4** (the *gra* cluster) (Sherman et al., 1989; Bechtold et al., 1995; Ichinose et al., 1998a) and medermycin (MED) **5** (the *med* cluster) (Ichinose et al., 2003). Comparative analysis of the three clusters revealed the unexpected lack of an *actVA-ORF6* homolog in the *gra* and *med* clusters, even though oxygen is found at the C-6 position in both GRA **4** and MED **5**. Instead, they include oxygenase genes (*gra-ORF21* and *med-ORF7*, respectively) homologous to *actVA-ORF5*, which was initially deduced to encode a hydroxylase for the C-8 position (Caballero et al., 1991) based on its significant similarity (>70%) to *pheA* encoding a phenol hydroxylase from *Bacillus stearothermophilus* (Kim and Oriel, 1995). Recently, ActVA-ORF5 was reported to form a two-component monooxygenase together with a flavin: NADH oxidoreductase, ActVB, which provides reduced flavin to the actual oxygenase component conducting the C-8 oxygenation in ACT biosynthesis (Valton et al., 2004, 2006). The *gra* and *med* clusters also contain genes homologous to *actVB* (*gra-ORF34* and *med-ORF13*, respectively). The absence of the hydroxyl group at C-8 of MED **5** as well as the lack of an *actVA-ORF6* homolog in the *med* cluster prompted us to propose the possible involvement of Med-ORF7, an ActVA-ORF5 homolog, in C-6 oxygenation in MED biosynthesis (Ichinose et al., 2003). These conflicting situations raise questions about the *in vivo* contributions of the ActVA-ORF5/ActVB and ActVA-ORF6 oxygenases to ACT biosynthesis. This paper describes a functional analysis of the *actVA-ORF5*, *actVA-ORF6*, and *actVB* genes based on molecular genetics, metabolic analysis, and biochemical characterization, revealing a novel

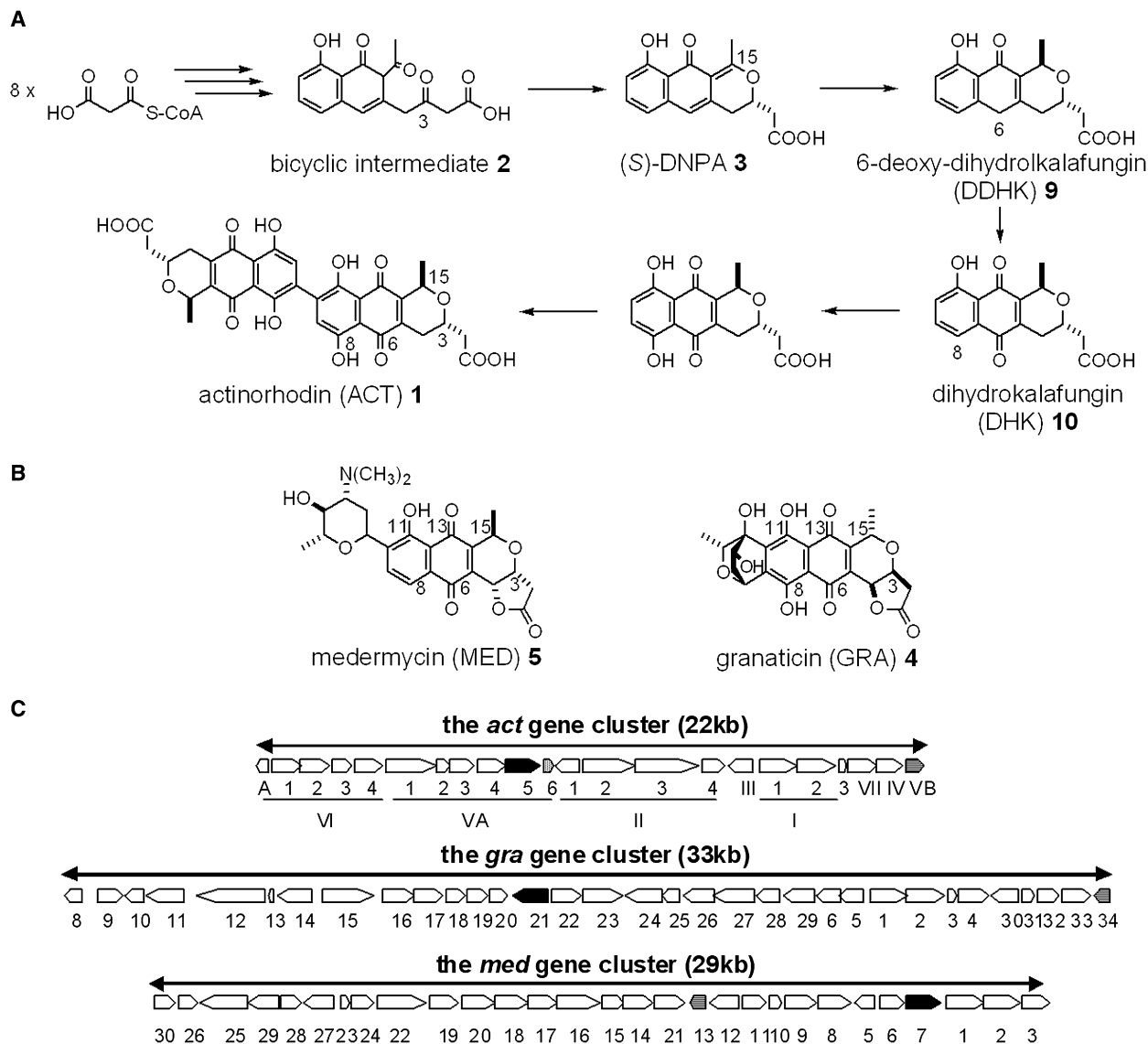


Figure 1. The Overview of BIQ Biosyntheses

(A) The proposed later tailoring steps of the ACT biosynthetic pathway. The numbers are based on the biosynthetic order.

(B) The structures of benzoisochromanquinone (BIQ) antibiotics.

(C) The biosynthetic gene clusters of ACT, granaticin, and medermycin. *actVA*-ORF6 is shown by a dotted arrow. *actVA*-ORF5 and its homologs are shown by filled arrows. The *actVB* homologs are shown by striped arrows.

situation in which alternative pathways are available for the later tailoring steps of ACT biosynthesis.

RESULTS

actVA-ORF5, but Not *actVA*-ORF6, Is Essential for ACT Biosynthesis

To establish the *in vivo* function of *actVA*-ORF5 and ORF6, we constructed deletion mutants for these genes. In the *act* cluster, the extreme 3' end of *actVA*-ORF5 overlaps with the 5' end of *actVA*-ORF6, indicative of potential translational coupling. Inactivation of *actVA*-ORF5 would have polar effects on the downstream gene, *actVA*-ORF6. Therefore, we initially inactivated

both genes by replacing them with a spectinomycin-streptomycin-resistance (*aadA*) cassette, resulting in a $\Delta actVA$ -5,6 double mutant (see Figure S1 article online). Correct disruption of the genes was confirmed by Southern blot analysis (Figure S1). A strain (M510) wild-type for the ACT pathway produced ACT **1** and its lactonized derivatives (ACTs): γ -actinorhodin (γ -ACT) **6** and γ' -actinorhodin (γ' -ACT) **7**, as shown in Figure 2. The $\Delta actVA$ -5,6 mutant did not produce ACTs (**1**, **6**, and **7**) at all. Instead, the mutant accumulated a yellowish-brown pigment, demonstrating the involvement of *actVA*-ORF5 and/or *actVA*-ORF6 in ACT biosynthesis (Figures 2A and 2C). Our previous spectral analysis elucidated its structure as a novel perylenequinone-type shunt product, 7*H*,16*H*-perilo

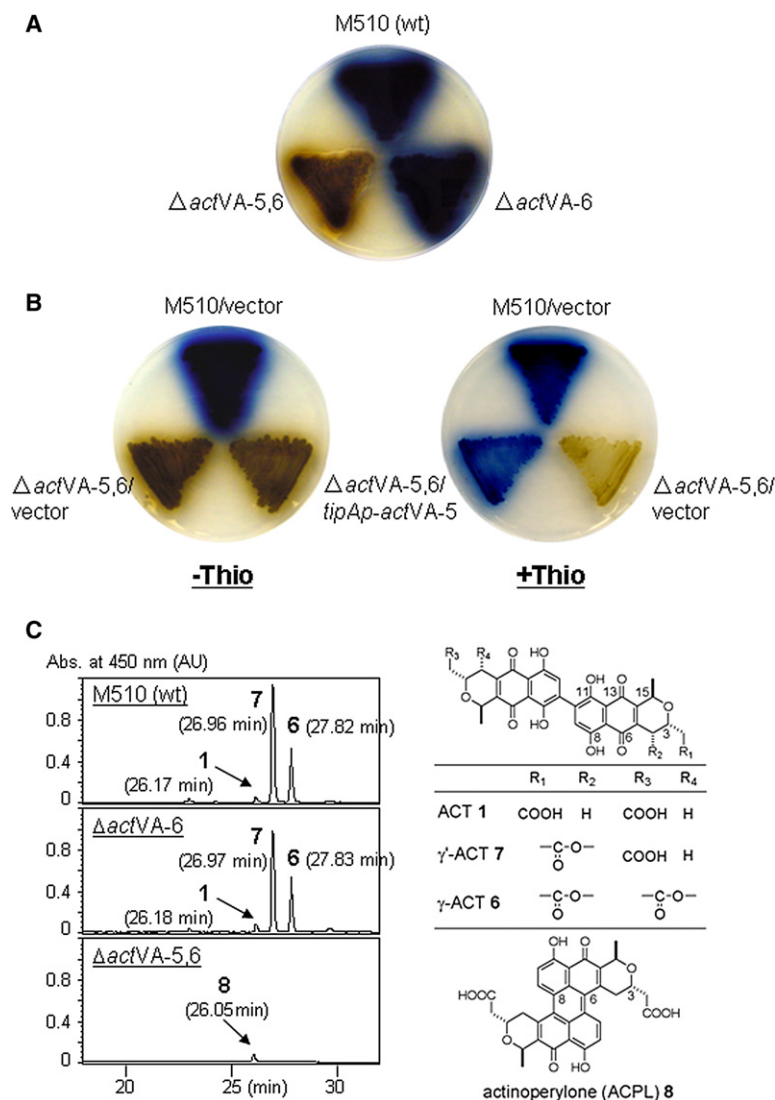


Figure 2. Functional Analysis of *actVA*-ORF5 and ORF6

(A) Effect of the *actVA* deletion mutations on ACT biosynthesis. Strains were inoculated on R5⁻ medium and grown at 30°C for 4 days. The reverse side of plates is shown.

(B) Complementation of the Δ*actVA*-5,6 mutant. The *actVA*-ORF5 gene was expressed by using pJ8600+*actVA5*. Strains were grown on R5⁻ medium at 30°C for 3 days, either in the absence (-Thio) or presence (+Thio) of thiostrepton (10 μg/ml).

(C) HPLC chromatograms of the ACT-related metabolites from culture medium of the strain M510 and its *actVA* mutants. Strains were cultured in R5MS medium, and the ACT-related metabolites in the culture supernatants were analyzed as described in Experimental Procedures. Chemical structures of the relevant compounds are shown on the right side of the panel.

possible that a presumptive homolog of *actVA*-ORF6 exists elsewhere in the genome and compensated for the mutation. However, genomic sequence analysis of *S. coelicolor* A3(2) (Bentley et al., 2002) revealed no homologs of *actVA*-ORF6, at least from the view of amino acid sequence homology. Furthermore, it has been demonstrated that the *act* cluster contains all genetic information required for ACT biosynthesis (Malpartida and Hopwood, 1984). Apparently, *actVA*-ORF5, but not *actVA*-ORF6, is essential for ACT biosynthesis, and the C-6 oxygenation step in ACT biosynthesis should be mainly governed by *actVA*-ORF5.

In Vivo Contribution of ActVA-ORF5/ActVB and ActVA-ORF6 as the C-6 Monooxygenase

A flavin:NADH oxidoreductase, ActVB, has been reported to be necessary for ActVA-ORF5 to function as a monooxygenase in vitro, and a combination of the two proteins was named the ActVA-

ActVB system (Valton et al., 2004, 2006). In our study, a more precise designation, the ActVA-ORF5/ActVB system, is proposed. To clarify the in vivo function of *actVB*, this gene was replaced by an erythromycin-resistance (*ermE*) cassette as described in Experimental Procedures (Figure S3). HPLC analyses of culture supernatants clearly showed that the deletion mutant, Δ*actVB*, produced ACTs (6 and 7) and ACPL 8 simultaneously (Figure 3). Quantitative estimations demonstrated that the total amount of ACTs (6 and 7) produced was decreased to about 30% of wild-type levels made by M510. The amount of ACPL 8 was almost the same as in the Δ*actVA*-5,6 mutant. This result indicates that deletion of *actVB* perturbed the ActVA-ORF5/ActVB system and led to interruption of efficient C-6 oxygenation of DDHK 9. Previously, an *actVB* mutant strain, B135 (Rudd and Hopwood, 1979), was reported to produce kalafungin (KAL) 14 (Cole et al., 1987). Under our culture conditions, however, the strain B135 was confirmed to produce γ-ACT 6 and ACPL 8, consistent with the results from our Δ*actVB* mutant, and neither KAL 14 nor dihydrokalafungin (DHK) 10 could be detected (data not shown).

[2,1c:8,7-*c'*]dipyran-7,16-dione,1,3,4,9,11,12-hexahydro-8,15-dihydroxy-1*R*,9*R*-dimethyl-3*S*,11*S*-diacetic acid, which was designated as actinoperylone (ACPL) 8 (Taguchi et al., 2008). Blocking oxygenation at C-6 of 6-deoxy-dihydrokalafungin (DDHK) 9 would result in possible tautomerization to the dihydroxynaphthalene derivative, followed by oxidative dimerization to afford ACPL 8. Therefore, C-6 oxidation of DDHK 9 is deduced to be compromised in the Δ*actVA*-5,6 mutant.

Next, we deleted *actVA*-ORF6 alone to construct the mutant Δ*actVA*-6 (Figure S1), but no obvious effect of the mutation on ACT production was detected (~9% less production than the wild-type, WT) (Figures 2A and 2C), indicating a rather limited contribution of *actVA*-ORF6 to ACT biosynthesis. In addition, ectopic expression of *actVA*-ORF5 alone under the control of a thiostrepton-inducible promoter, *tipAp*, in the Δ*actVA*-5,6 mutant (the recombinant, Δ*actVA*-5,6/*actVA*-5) restored ACT production in response to thiostrepton induction (Figure 2B; Figure S2). In contrast, expression of *actVA*-ORF6 alone in the Δ*actVA*-5,6 mutant (the recombinant, Δ*actVA*-5,6/*actVA*-6) had no obvious effect on the metabolic profile (Figure S2). It was

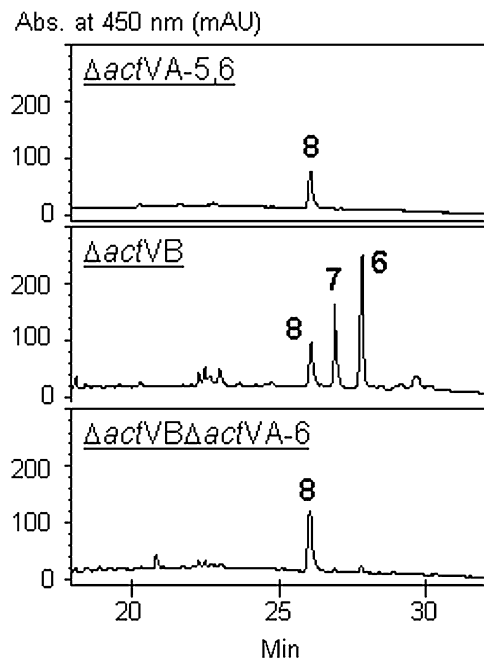


Figure 3. Effect of the $\Delta actVB$ and $\Delta actVB \Delta actVA-ORF6$ Double Mutations on ACT Biosynthesis

HPLC profiles monitored by absorbance at 450 nm are shown. The $\Delta actVB$ mutant produced ACTs (**6** and **7**) and ACPL **8** simultaneously, whereas the $\Delta actVB \Delta actVA-ORF6$ double mutant produced only ACPL **8**.

Given the crucial role of ActVB in the enzyme system, the $\Delta actVB$ mutation should be highly detrimental to the enzymatic function of the ActVA-ORF5/ActVB system. Nevertheless, the

mutant produced a significant amount of ACTs. Therefore, we decided to investigate the contribution of *actVA-ORF6* in this genetic background. For this purpose, we constructed a $\Delta actVB \Delta actVA-ORF6$ double mutant ($\Delta actVB \Delta actVA-6$). This mutant still accumulated ACPL **8** (Figure 3), but virtually no ACTs (**1**, **6**, and **7**), indicating that ActVA-ORF6 really catalyzes C-6 oxygenation, and that this manifestation of enzymatic activity depends on the $\Delta actVB$ mutation. In other words, C-6 oxygenation is normally governed by the ActVA-ORF5/ActVB system, and the ActVA-ORF6 protein contributes as an alternative C-6 monooxygenase in the *actVB* mutant background, in which the function of the highly efficient ActVA-ORF5/ActVB system is compromised.

In Vitro Activity of ActVA-ORF5/ActVB as a Quinone-Forming Oxygenase

The results described above strongly suggest that the ActVA-ORF5/ActVB system is a quinone-forming enzyme that converts DDHK **9** into DHK **10**. To demonstrate this enzymatic activity in vitro, we expressed and purified both ActVA-ORF5 and ActVB as His₆-tagged proteins (Figure S4). We also prepared His₆-tagged ActVA-ORF6 as a positive control. Because the presumptive natural substrate, DDHK **9**, is not available, we used emodinanthrone **11** as a model substrate (Figure 4). This compound was successfully used in previous studies of other quinone-forming enzymes (Chen et al., 1995), and its chemical structure is more analogous to that of DDHK **9** than tetracenomycin F1 (TCMF1) **13**, which was used in the biochemical studies of ActVA-ORF6 (Kendrew et al., 1997). ActVA-ORF5 and ActVB proteins were incubated with emodinanthrone **11** and cofactors FMN and NADH as described in Experimental Procedures. Strikingly, the reconstituted ActVA-ORF5/ActVB system catalyzed

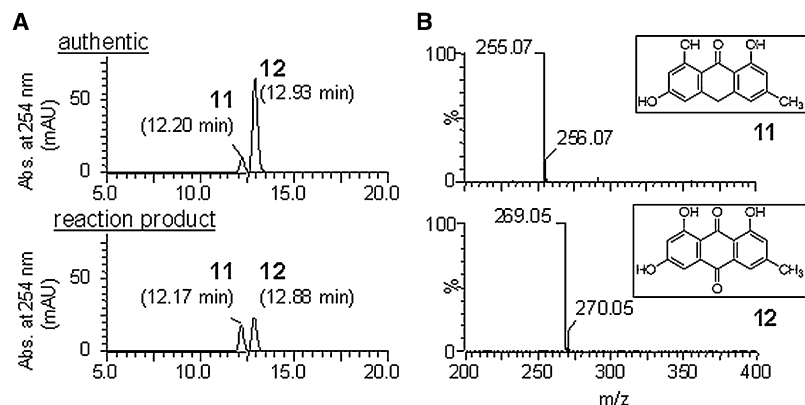
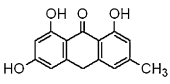
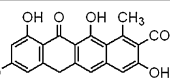


Figure 4. Demonstration of an In Vitro Quinone-Forming Monooxygenase Activity of the ActVA-ORF5/ActVB System

(A) HPLC analysis of reaction products. ActVA-ORF5 (1 μ M) and ActVB (100 nM) were incubated with emodinanthrone **11** (50 μ M) for 10 min at 25°C as described in Experimental Procedures. Elution profiles were monitored by absorbance at 254 nm. Top, authentic (0.5 μ g each) emodinanthrone **11** and emodin **12**; bottom, an ethyl acetate extract from an in vitro assay mixture.

(B) Mass spectra of emodinanthrone **11** and emodin **12** extracted from a reaction mixture. The peaks corresponding to emodinanthrone **11** (m/z 255 as $[M-H]^-$) and emodin **12** (m/z 269 as $[M-H]^-$) were detected.

(C) Kinetic properties of ActVA-ORF5/ActVB, ActVA-ORF6, and their related enzymes.

Substrate	Enzyme	K_m (μ M)	V_{max} (nmol/min/mg)	K_{cat} (s^{-1})	K_{cat}/K_m ($s^{-1}\mu M^{-1}$)	Reference
 emodinanthrone 11	ActVA-ORF5	7.54	164	7.01	0.930	This Study
	ActVA-ORF6	211	511	6.65	0.032	This Study
	AknX	39.8	73.5	-	-	Chung et al. (2002)
 tetracenomycin F1 13	ActVA-ORF6	4.8	200	2.5	0.521	Kendrew et al. (1997)
	TcmH	7.47	473	-	-	Shen and Hutchinson (1993)

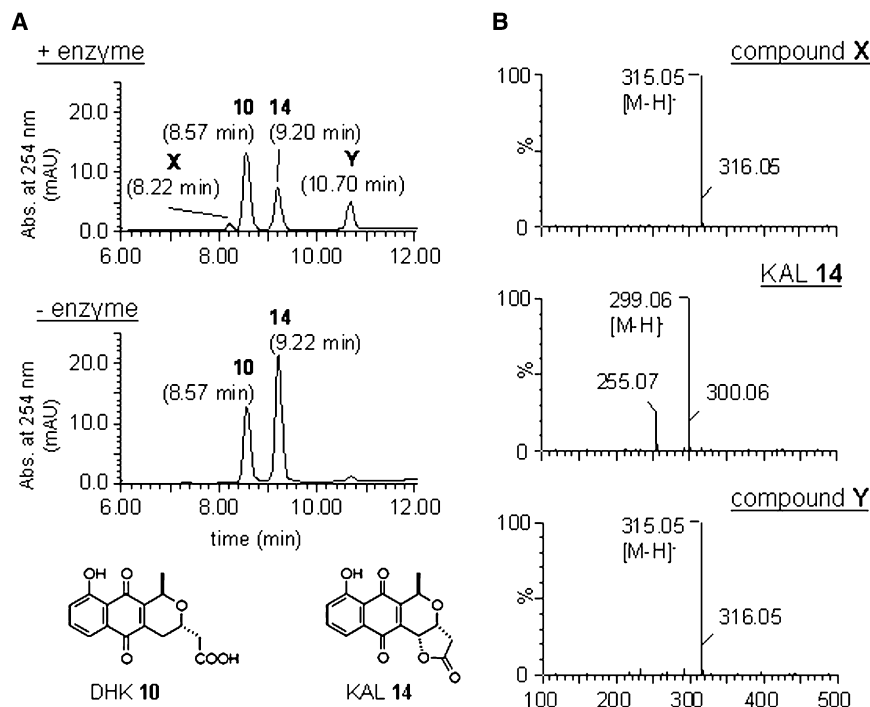


Figure 5. Demonstration of a DHK Oxygenation Activity of the ActVA-ORF5/ActVB System

(A) HPLC analysis of reaction products. Assay conditions were essentially the same as those used for emodinanthrone **11** (Figure 4). Top, DHK **10** (50 μ M) was incubated with ActVA-ORF5 and ActVB; bottom, DHK without the enzymes.

(B) Mass spectra of (X), KAL **14**, and (Y) extracted from a reaction mixture. The peaks corresponding to X, Y (m/z 315 as $[M-H]^-$), and KAL **14** (m/z 299 as $[M-H]^-$) were detected.

described in Experimental Procedures. Although these compounds were rapidly converted to their cognate quinone form by autoxidation, the ActVA-ORF5/ActVB system significantly enhanced this rate, confirming a quinone-forming activity of the enzyme system (Figure S5). However, no hydroxylation activity was detected in these assays (Figure S5).

Finally, therefore, we decided to use the presumptive natural substrate, DHK **10**, for C-8 hydroxylation to assess the

oxidation of emodinanthrone **11** to emodin **12**, demonstrating a quinone-forming activity of the system (Figures 4A and 4B). We confirmed, as shown by Valton et al. (2004, 2006), that ActVA-ORF5, the genuine oxygenase component, absolutely required ActVB, FMN, and NADH for its enzymatic activity (data not shown). In contrast, ActVA-ORF6 did not require any exogenously added cofactors, as described previously (Kendrew et al., 1997).

To characterize the enzymatic properties of the ActVA-ORF5/ActVB system, kinetic parameters were determined (Figure 4C). Interestingly, the K_m for emodinanthrone **11** of this enzyme system was significantly lower than that of ActVA-ORF6 (7.54 μ M versus 211 μ M) and comparable to that of AknX, a distant homolog of ActVA-ORF6 involved in aklavinone biosynthesis in *Streptomyces galilaeus* (Chung et al., 2002). These results imply more efficient oxidation of DDHK **9** by the ActVA-ORF5/ActVB system. Together, we unambiguously demonstrated an enzymatic activity of ActVA-ORF5/ActVB as a quinone-forming oxygenase.

An Additional Oxygenase Activity of the ActVA-ORF5/ActVB System

The ActVA-ORF5/ActVB system has been proposed to be involved in the C-8 hydroxylation step in ACT biosynthesis (Valton et al., 2006, 2008). Therefore, we then investigated this possibility. Our model substrate emodinanthrone **11** is suitable to detect a quinone-forming activity because of its intrinsic slow rate of autoxidation. However, this compound **12** is unlikely to be hydroxylated at position 4 (equivalent to C-8 of ACT), owing to its highly substituted nature. Thus, we used less substituted anthracenes, anthrone, and dihydranthrone to detect quinone formation and subsequent hydroxylation. These model substrates were assessed under our standard assay conditions as

involvement of the ActVA-ORF5/ActVB system in this biosynthetic step. Results of assays are shown in Figure 5. DHK **10** is spontaneously lactonized, possibly via a hydroquinone form, to KAL **14** (Ichinose et al., 1998b), which was detected irrespective of the presence of the enzyme system (Figure 5A). Strikingly, the reaction with the enzyme system provided new compounds X and Y (Figure 5A), and their molecular mass was shown to be 315 (ESI-negative) (Figure 5B), implying that these compounds are oxygenated molecules of KAL **14**. It is likely that these compounds are generated by C-8 or C-10 hydroxylation catalyzed by the ActVA-ORF5/ActVB monooxygenase system. Based on the significant decrease of KAL **14** in the enzymatic sample, this compound is suggested to be the actual substrate for oxygenation to produce the compounds X and Y. Although further structural elucidation is required, we clearly demonstrated that the ActVA-ORF5/ActVB system possesses an additional oxygenation activity other than the quinone-forming activity we discovered.

Shunt Pathway Leading to 8 in Relation to C-6 Oxygenation

A proposed scheme (Taguchi et al., 2008) for the formation of ACPL **8** includes oxidative coupling of DDHK **9**, which is the postulated product of a reductase, ActVI-ORF2 (Taguchi et al., 2000) (Figure 7). To elucidate the essential genes for the shunt pathway to ACPL **8**, we analyzed the *act* cluster-deficient strain, CH999, carrying plasmid-borne copies of the *act* biosynthetic genes required for the formation of (S)-DNPA **3**, with actVI-ORF2 in addition (CH999/pIJ5659) (Ichinose et al., 1999). HPLC analysis of a liquid culture of CH999/pIJ5659 clearly detected ACPL **8** (Figure 6). This result proves that actVI-ORF2 indeed encodes a reductase for C-15, and, most importantly, formation of ACPL **8** was demonstrated by the minimal gene

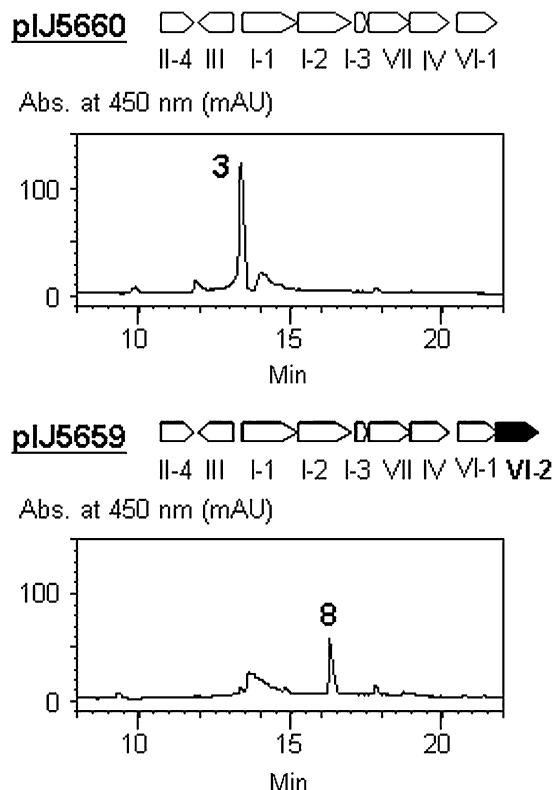


Figure 6. Formation of Actinoperlyone by the Minimal Gene Set

HPLC analyses of metabolites produced by *S. coelicolor* CH999 recombinants harboring either pIJ5660 or pIJ5659. Chromatograms monitored by absorbance at 450 nm are shown. The gene sets used for the plasmids are also shown above each chromatogram. The recombinant strain harboring pIJ5660 produced (S)-DNPA **3**. On the other hand, the strain harboring pIJ5659 accumulated a shunt product, ACPL **8**.

sets for the possible formation of DDHK **9**. Interruption of the C-6 oxygenation of DDHK **9** would result in possible tautomerization to the dihydroxynaphthalene derivative, followed by oxidative dimerization to afford ACPL **8**. One of the possible candidates involved in the coupling is a P450 gene (Zhao et al., 2007) outside the *act* cluster.

DISCUSSION

Oxidative modifications catalyzed by monooxygenases are common tailoring steps in the biosynthesis of polyketide metabolites, including both aromatic and macrocyclic antibiotics. The most extensively studied examples are the cytochrome P450-dependent monooxygenases (Munro et al., 2007). However, the 22 kb *act* biosynthetic gene cluster carries no genes for P450-type enzymes, suggesting that distinct kinds of monooxygenases are involved in the oxygenation steps at C-6 and C-8 in ACT biosynthesis.

ActVA-ORF6 significantly resembles the monooxygenase encoded by *tcmH* involved in tetracenomyacin (TCM) biosynthesis in *Streptomyces glaucescens* (Shen and Hutchinson, 1993). Because TcmH had been shown to be a quinone-forming monooxygenase that converts TCMF1 **13** to TCMD3, it was

reasonable to assume that ActVA-ORF6 catalyzes the C-6 oxygenation of DDHK **9** (Fernández-Moreno et al., 1994). Indeed, Kendrew et al. (1997) demonstrated its quinone-forming activity by using TCMF1 **13** as a model substrate. Furthermore, the crystal structure of ActVA-ORF6 in complex with substrate and product analogs provided an explanation for C-6 oxygenation, where the active site cavity of the enzyme acts as a shield for the substrate, DDHK **9**, leaving only the C-6 carbon exposed to molecular oxygen (Sciara et al., 2003).

Although C-6 oxygenation is a tailoring step common to all BIQ biosyntheses, neither the *gra* nor *med* cluster possesses *actVA*-ORF6 homologs (Figure 1C). This prompted us to investigate the *in vivo* contribution of *actVA*-ORF6 to ACT production. An *actVA*-ORF6 deletion mutant produced ACTs at levels only slightly less than the wild-type, suggesting a rather limited contribution of the gene to ACT biosynthesis (Figure 2). Instead, the gene immediately upstream, *actVA*-ORF5, was found to be critical for C-6 oxygenation in the present study (Figures 2 and 4). The *actVA* genetic region corresponds to one of the phenotypic classes of blocked mutants that produce diffusible brown pigments (Rudd and Hopwood, 1979). Most of the *actVA* mutations were mapped to the *actVA*-ORF5 gene (Caballero et al., 1991), and later chemical characterization of an *actVA*-ORF5 mutant (strain B1) carrying the *act*-101 mutation (Caballero et al., 1991) identified (S)-DNPA **3** as an *actVA* intermediate (Cole et al., 1987). We also analyzed the same class of *actVA*-ORF5 mutant (strain B9) carrying the *act*-109 mutation (Caballero et al., 1991) and identified ACPL **8** as a major ACT-related metabolite, but a trace amount of (S)-DNPA **3**, though no ACTs (**1**, **6**, and **7**), was also detected (data not shown). These results demonstrated the critical role of *actVA*-ORF5 in C-6 oxygenation. Consistent with this conclusion, the *gra* and *med* clusters carry homologs of *actVA*-ORF5, *gra*-ORF21 (Ichinose et al., 1998a), and *med*-ORF7 (Ichinose et al., 2003).

The *actVB* gene was initially identified genetically among *actV* mutants, being phenotypically similar but not identical to the *actVA* mutants (Rudd and Hopwood, 1979; Fernández-Moreno et al., 1992). Based on the isolation of KAL **14**, which is convertible *in vivo* to ACT **1** (Cole et al., 1987), *actVB* had been postulated to be involved in oxidative dimerization in ACT biosynthesis. Despite an apparent lack of an equivalent biosynthetic step, we discovered *actVB* homologs (*gra*-ORF34, *med*-ORF13) in the other BIQ gene clusters (Ichinose et al., 1998a, 2003) (Figure 1C), indicating their role in a step common to the biosynthesis of these undimerized compounds. The ActVB protein was shown to be a flavin:NADH oxidoreductase (Kendrew et al., 1995). Recently, the ActVA-ORF5 and ActVB proteins were reported to constitute a two-component monooxygenase system, in which ActVB donates reduced flavin to the actual oxygenase component, ActVA-ORF5 (Valton et al., 2004), providing an explanation for the copresence of their cognate genes in all BIQ pathways. Detailed biochemical studies (Valton et al., 2008) proposed the involvement of the ActVA-ORF5/ActVB system in the oxygenation step at C-8 in ACT biosynthesis. However, notwithstanding the absence of the hydroxyl group at C-8 in MED **5**, highly conserved orthologs of *actVA*-ORF5 (*med*-ORF7) and *actVB* (*med*-ORF13) are present in the *med* gene cluster. This fact implies an additional function for the ActVA-ORF5/ActVB system other than as a catalyst for C-8

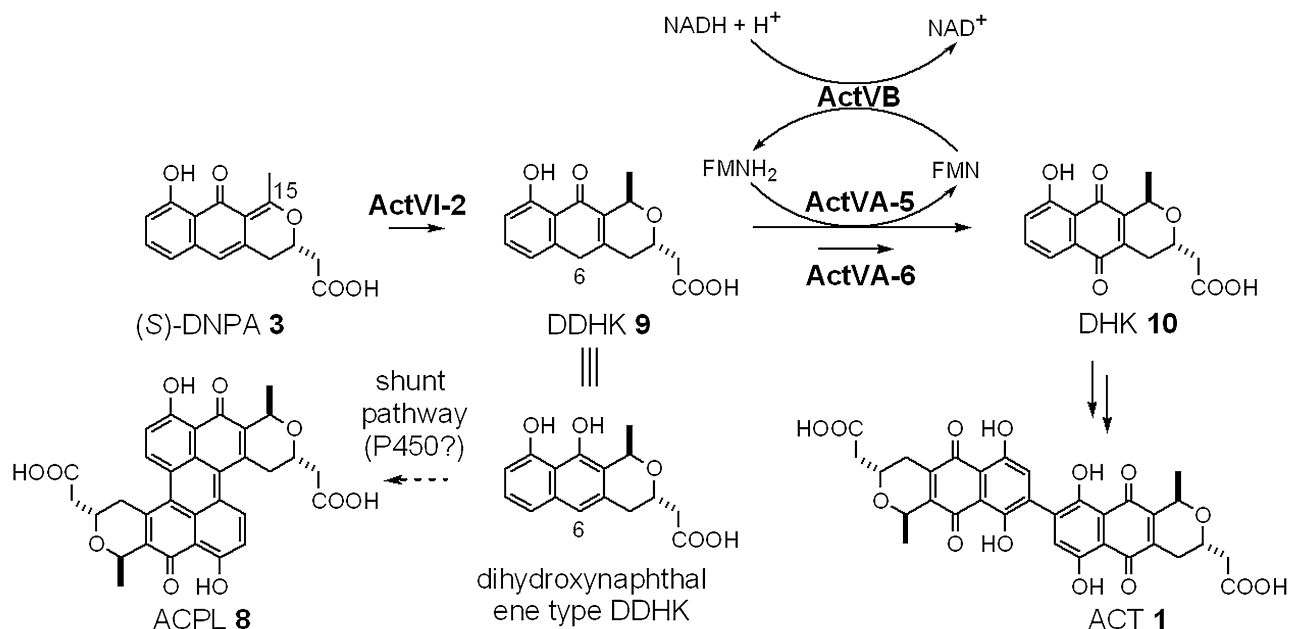


Figure 7. Proposed Later Tailoring Pathway of ACT Biosynthesis

The ACT biosynthetic pathway exploits a dual enzyme system for the C-6 oxygenation of DDHK **9**. The ActVA-ORF5/ActVB system is a principal enzyme for this reaction. The ActVA-ORF6 protein also catalyzes the same reaction, but its contribution is rather limited in the wild-type genetic background. However, the activity of ActVA-ORF6 is manifested in the *actVB* genetic backgrounds. Production of ACT **1** from DHK **10** requires at least two reaction steps: dimerization and 8-hydroxylation.

hydroxylation. Indeed, we demonstrated the involvement of ActVA-ORF5/ActVB in the C-6 oxygenation step.

We further investigated the *in vivo* contributions of the ActVA-ORF5/ActVB and ActVA-ORF6 monooxygenases by constructing an *actVB* deletion mutant ($\Delta actVB$). This mutant was expected to produce ACPL **8**, owing to a lack of the principal C-6 monooxygenase, ActVA-ORF5/ActVB. In fact, the $\Delta actVB$ mutant accumulated ACPL **8** (Figure 3), but still produced a considerable amount of ACTs (**6** and **7**), indicating two possibilities: (i) ActVA-ORF5 itself is partially functional without ActVB; (ii) ActVA-ORF6 makes a significant contribution in the $\Delta actVB$ genetic background. To clarify this issue, we then prepared an *actVB actVA-ORF6* double mutant ($\Delta actVB \Delta actVA-6$), and we confirmed that ACT production was virtually abolished in this mutant, although the accumulation of ACPL **8** was still observed (Figure 3). The results clearly indicate that ActVA-ORF6 is also functional *in vivo* and that its activity as a C-6 monooxygenase is manifested in the *actVB* mutant, in which the function of the ActVA-ORF5/ActVB system is compromised.

Following the *in vivo* experiments, we attempted to prove an *in vitro* quinone-forming activity of the ActVA-ORF5/ActVB system. We could readily reconstitute the two-component system with purified recombinant proteins and detect its enzymatic activity by using emodinanthrone **11** as a model substrate (Figure 4). A quinone-forming activity of the ActVA-ORF6 protein was also confirmed in our assay system. These observations reinforce our claim that the ActVA-ORF5/ActVB system is the principal C-6 monooxygenase in ACT biosynthesis.

It is interesting that ActVA-ORF6 has a lower K_m for tetracyclic mycin F1 (TCMF1) **13** than for a substrate closer in structure to an ACT intermediate, and that it is present only in the ACT system,

even though GRA and MED biosynthesis also requires C-6 oxygenation. Perhaps the *actVA-ORF6* gene has been acquired by horizontal gene transfer from an unknown source, now providing an alternative route to C-6 oxygenation.

An immediate interest would be the possible involvement of the ActVA-ORF5/ActVB system not only in C-6 oxygenation, but also in C-8 hydroxylation, as proposed previously (Valton et al., 2006, 2008). Under our assay conditions, the model anthrone substrates (emodinanthrone **11**, anthrone, and dithranol) were efficiently converted to the corresponding anthraquinones, but they did not receive any additional oxygenation. Therefore, we used the presumptive natural substrate, DHK **10**. As expected, this compound was readily converted to the oxygenated compounds (Figure 5), which possess the molecular mass (316) corresponding to hydroxylated KAL **14**. Previous studies on the ActVA-ORF5/ActVB system (Valton et al., 2006) demonstrated its *in vitro* oxygenating activity that catalyzes the conversion of DHK **10** to its monooxygenated derivative, DHK-OH, with a molecular mass of 318. This conversion was, however, less efficient, and the true substrate was suggested to be the hydroquinone form of DHK **10**, which was efficiently oxygenated under the anaerobic assay conditions employed (Valton et al., 2006). Our experimental data imply that KAL **14**, but not DHK **10**, is the actual substrate for this enzymatic reaction (Figure 5). Although further studies are required to determine the *bona fide* biosynthetic substrate for the hydroxylation reaction and the chemical structure of the reaction products, we demonstrated unambiguously an additional oxygenation activity other than the quinone-forming activity of the ActVA-ORF5/ActVB system.

The shunt formation of ACPL **8** by the *actVA-ORF5* or *actVB* mutants is reasonably explained by oxidative coupling of

DDHK 9, a postulated substrate of C-6 oxygenation. Strikingly, the recombinant strain with the expression plasmid (pIJ5659) carrying the minimal set of genes for the formation of DDHK 9 produced ACPL 8, clearly suggesting a direct link between interruption of C-6 oxygenation and oxidative coupling.

The combined data allow us to propose an alternative oxygenation pathway in ACT biosynthesis as shown in Figure 7, including a dual C-6 oxygenation system consisting of ActVA-ORF5/ActVB and ActVA-ORF6. Our experimental results do not disprove the functional assignment of the ActVA-ORF5/ActVB system as a C-8 hydroxylase. Neither the missense *actVA-ORF5* mutant (strain B9; unpublished data) nor the *ΔactVA-5,6* mutant harboring the *actVA-ORF6* expression plasmid produced any ACTs (1, 6, and 7), although the alternative C-6 monooxygenase ActVA-ORF6 is highly likely to be functional in these strains. Thus, it is apparent that the ActVA-ORF5 protein is involved in an additional biosynthetic step after C-6 oxygenation. Indeed, we confirmed an additional function of the ActVA-ORF5/ActVB system other than that as a quinone-forming enzyme. Further genetic and chemical studies are in progress to elucidate details of the late ACT biosynthetic pathway, including the C-8 hydroxylation step.

SIGNIFICANCE

The striking conclusion from this work is that the gene cluster for ACT biosynthesis encodes two alternative routes for quinone formation at a critical stage in post-PKS tailoring. One of these, catalyzed by ActVA-ORF5/ActVB, is the major route in the wild-type, but when *actVB* is deleted (and perhaps when the expression level of *actVB* is low in the wild-type), the alternative route, catalyzed by ActVA-ORF6, becomes manifested. Oxygenation, including quinone formation and hydroxylation, is one of the key steps in secondary metabolism; thus, these findings may have wide significance for understanding and manipulating the oxygenation of a variety of aromatic compounds. The possible bifunctionality of the ActVA-ORF5/ActVB system found in this study would open the possibility of its application to the oxygenation of various aromatic compounds.

EXPERIMENTAL PROCEDURES

Bacterial Strains

S. coelicolor M510 (M145 *ΔredD*) (Floriano and Bibb, 1996) was used as the wild-type strain throughout this study. This strain does not produce the red-pigmented prodiginines due to the *ΔredD* mutation, allowing for easy characterization of *act* mutants. *S. coelicolor* CH999 (*proA1 argA1 redE60 Δact::ermE SCP1⁻ SCP2⁻*) (McDaniel et al., 1993) was also used in some experiments. *Streptomyces lividans* TK21, *Escherichia coli* DH5 α , and *E. coli* GM2163 (*dam⁻ dcm⁻*) were used for routine DNA manipulation. *E. coli* BL21(DE3)/pLysS was used as the host for protein expression. *Streptomyces tanashiensis* JCM4086 (RIKEN) was used for the isolation of DHK.

DNA Manipulation

Plasmid isolation, restriction enzyme digestion, ligation, and transformation of *E. coli* and *Streptomyces* were performed as described previously (Kieser et al., 2000; Sambrook et al., 1989). PCR was performed with LA Taq (TaKaRa, Japan) or KOD -Plus- (Toyobo, Japan) DNA polymerase. PCR primers used in this study are listed in Table S1.

Construction of the *ΔactVA-5,6*, *ΔactVA-6*, and *ΔactVB* Mutants

The *ΔactVA-5,6* Mutant

A 1 kb region 5' of *actVA-ORF5* was amplified by PCR with primers $\Delta actVA5,6-UF$ and $\Delta actVA5,6-UR$. A second 1.1 kb region 3' of *actVA-ORF6* was amplified with primers $\Delta actVA6-DF$ and $\Delta actVA6-DR$. The PCR fragments were inserted between the EcoRI and HindIII sites of pUC19 by three-fragment ligation, yielding pUC19+ $\Delta actVA5,6$. The *aadA* gene was amplified from pIJ2059 (Kieser et al., 2000) by using primers *aadA-F* and *aadA-R*. The amplified *aadA* gene cassette was cloned in the XbaI site of pUC19+ $\Delta actVA5,6$, generating pUC19+ $\Delta actVA5,6::aadA$. The $\Delta actVA5,6::aadA$ construct was excised by digestion with EcoRI and HindIII and was ligated with pGM9 (Kieser et al., 2000), which had been treated with the same enzymes. The ligation mixture was used to transform *S. lividans* TK21 protoplasts to yield the plasmid pGM9+ $\Delta actVA5,6::aadA$. *S. coelicolor* M510 was transformed with pGM9+ $\Delta actVA5,6::aadA$, and transformants were selected with thiostrepton (Thio). To obtain single-crossover recombinants, purified transformants were cultured on Thio-containing plates at 37°C. Because pGM9 carries a temperature-sensitive replicon of pSG5, it cannot replicate at this temperature. Thio-resistant single-crossover recombinants were subcultured by two rounds of streaking in the absence of Thio at 37°C. Double-crossover recombinants ($\Delta actVA-5,6$) in which the delivery plasmid was lost from cells were identified as colonies with Thio-sensitive and streptomycin-resistant phenotypes. The correct deletion of the genes was confirmed by PCR and Southern blot analyses.

The *ΔactVA-6* Mutant

A 1 kb region 5' of *actVA-ORF6* was amplified by PCR with primers $\Delta actVA6-UF$ and $\Delta actVA6-UR$. A 1.1 kb region 3' of *actVA-ORF6* was amplified as described above. These PCR fragments were inserted between the EcoRI and HindIII sites of pUC19 by three-fragment ligation, generating pUC19+ $\Delta actVA6$. The *aadA* gene cassette described above was cloned in this recombinant plasmid, yielding pUC19+ $\Delta actVA6::aadA$. The $\Delta actVA6::aadA$ construct was excised by digestion with EcoRI and HindIII and ligated with pGM9 to obtain pGM9+ $\Delta actVA6::aadA$. The resulting plasmid was introduced into *S. coelicolor* M510, and the *actVA-ORF6* deletion mutant ($\Delta actVA-6$) was obtained as described above.

The *ΔactVB* Mutant

A 1 kb region 5' of *actVB* was amplified with primers $\Delta actVB-UF$ and $\Delta actVB-UR$. A second 1 kb region 3' of *actVB* was amplified with primers $\Delta actVB-DF$ and $\Delta actVB-DR$. The PCR fragments were inserted between the EcoRI and XhoI sites of pGEM-11zf by three-fragment ligation, yielding pGEM+ $\Delta actVB$. The erythromycin/lincosycin-resistance gene, *ermE*, was excised from pIJ4026 (Kieser et al., 2000) by digestion with KpnI and was ligated with pGEM+ $\Delta actVB$, which had been treated with the same enzyme, generating pGEM+ $\Delta actVB::ermE$. The $\Delta actVB::ermE$ construct was recovered by digestion with EcoRI and XhoI and ligated with pGM9 to obtain pGM+ $\Delta actVB::ermE$. This plasmid was introduced into *S. coelicolor* M510, and the *actVB* deletion mutant ($\Delta actVB$) was screened by virtue of Thio-sensitive and lincosycin-resistance phenotypes. Similarly, pGM+ $\Delta actVB::ermE$ was introduced into the $\Delta actVA6$ mutant, and the $\Delta actVB \Delta actVA-ORF6$ double mutant ($\Delta actVB \Delta actVA6$) was obtained in analogous fashion.

Southern Hybridization

DNA fragments from agarose gels were transferred to Hybond-N+ nylon membrane (GE Healthcare). Probes were prepared by PCR with the following primer sets: *actVA5,6* probe, $\Delta actVA5,6-Pro-F$, and $\Delta actVA5,6-Pro-R$; *aadA* probe, *aadA-F*, and *aadA-R*; *actVB* probe, $\Delta actVB-Pro-F$, and $\Delta actVB-Pro-R$; *ermE* probe, *ermE-F*, and *ermE-R*. These probes were nonradioactively labeled by using the DIG DNA labeling kit (Roche). Hybridization, washing, and detection were performed as recommended by the manufacturer (Roche).

Plasmids

The plasmids used for complementation of the $\Delta actVA-5,6$ mutant were constructed as follows. The *actVA-ORF5* gene was amplified with the primers *actVA5-Nde* and *actVA5-Bam*. The NdeI-BamHI fragment was inserted into the *Streptomyces* expression plasmid pJ8600 (Kieser et al., 2000) that has the Thio-inducible *tipA* promoter, generating pJ8600+*actVA5*. Similarly, the *actVA-ORF6* gene was amplified with the primers *actVA6-Nde* and

actVA6-EcoXba. After digestion with NdeI and XbaI, the PCR product was cloned into pJ8600, yielding pJ8600+actVA6.

The *E. coli* expression plasmids used for purification of recombinant proteins were constructed as follows. The actVA-ORF5 gene was excised from pJ8600+actVA5 as the NdeI-BamHI fragment and cloned into pET-19b. The resulting plasmid, pET-actVA5, attaches the N-terminal His-tag sequence. Plasmid pET-actVA6 was constructed by using the DNA fragment amplified with primers actVA6-Nde and actVA6-Xho. The NdeI-XhoI fragment was inserted into pET-22b. The resulting plasmid, pET-actVA6, attaches the C-terminal His-tag sequence. The actVB gene was amplified with primers actVB-Nde and actVB-Bam, and the PCR fragment was cloned into pET-19b, yielding pET-actVB.

Culture Conditions for Production of ACT-Related Metabolites

Seed cultures (10 ml) were grown in TSB medium (Kieser et al., 2000) on a rotary shaker at 220 rpm and 30°C for 2 days. An aliquot (2 ml) of the seed culture was inoculated to 50 ml R5MS medium (consisting of 10 g/l glucose, 5 g/l yeast extract [Difco], 0.1 g/l casamino acids, 0.25 g/l K₂SO₄, 10.12 g/l MgCl₂·6H₂O, 5.73 g/l TES buffer, 2 ml/l trace element solution [pH 7.2]) in a 500 ml Erlenmeyer flask, and the culture was grown with shaking (220 rpm) at 30°C for 4 days. R5⁻ medium (Huang et al., 2001) was used for solid cultures.

HPLC Analysis

An aliquot of culture (1 ml) was centrifuged at 13,200 × g for 5 min. The supernatant (100 μl) was directly subjected to reversed-phase HPLC analysis on a Waters Multisolute System under the following conditions: column, TSK gel ODS-100V (4.6 id × 150 mm, TOSO); column temperature, 40°C; gradient elution, solvent A (0.5% acetic acid in CH₃CN) and solvent B (0.5% acetic acid in deionized H₂O); gradient profile: 0–35 min, 10%–94% A; 35–40 min, 94% A; 40–45 min, 94%–10% A; flow rate, 1.0 ml/min; detection, absorption between 250 and 600 nm using a photo-diode array detector (Waters 2996, Waters).

Expression and Purification of Recombinant ActVA-ORF5, ActVA-ORF6, and ActVB Proteins

His-ActVA-ORF5

E. coli BL21(DE3)/pLysS harboring pET-actVA5 was grown at 37°C to an OD₆₀₀ of 0.7 in 100 ml LB medium containing 0.2% glucose, 50 μg/ml ampicillin, and 25 μg/ml chloramphenicol (LBGAC). Expression was induced with 1 mM isopropyl-β-D-thiogalactopyranoside (IPTG), and incubation was continued at 37°C for an additional 3 hr. Cells were collected by centrifugation and stored at –70°C. The cell pellet was resuspended in buffer A (20 mM sodium phosphate [pH 7.4], 500 mM NaCl, 100 mM imidazole, 2 mM dithiothreitol, 0.1% CHAPS) containing Complete protease inhibitor cocktail (Roche) and sonicated. Insoluble material was removed by centrifugation, and the crude cell extract was chromatographed on a 1 ml HisTrap HP column (GE Healthcare) equilibrated with buffer A. Then, the column was washed with buffer A containing 300 mM imidazole, and the His-ActVA-ORF5 protein was eluted with 500 mM imidazole in the same buffer. The fractions containing His-ActVA-ORF5 were pooled and dialyzed against a buffer containing 20 mM Tris-HCl (pH 7.5), 2 mM dithiothreitol, 0.1% CHAPS, and 10% (w/v) glycerol. Protein concentration was determined by the Bradford procedure. Aliquots of the purified protein were stored at –70°C.

ActVA-ORF6-His

E. coli BL21(DE3)/pLysS transformed with pET-actVA6 was grown at 37°C to an OD₆₀₀ of 0.7 in 100 ml LBGAC medium. Expression was induced with 1 mM IPTG, and incubation was continued at 37°C for an additional 3.5 hr. Cells were harvested by centrifugation and stored at –70°C. The cell pellet was resuspended in buffer B (20 mM sodium phosphate [pH 7.4], 500 mM NaCl, 20 mM imidazole, 1 mM dithiothreitol, 10% (w/v) glycerol) containing Complete protease inhibitor cocktail and sonicated. After centrifugation, the crude cell extract was chromatographed on a 1 ml HisTrap HP column equilibrated with buffer B. Then, the column was washed with buffer B containing 100 mM imidazole, and the ActVA-ORF6-His protein was eluted with 300 mM imidazole in the same buffer. The fractions containing ActVA-ORF6-His were pooled and dialyzed against a buffer containing 20 mM Tris-HCl

(pH 7.5), 1 mM dithiothreitol, and 20% (w/v) glycerol. Aliquots of the purified protein were stored at –70°C.

His-ActVB

E. coli BL21(DE3)/pLysS harboring pET-actVB was grown at 37°C to an OD₆₀₀ of 0.3 in 100 ml LBGAC medium. Expression was induced with 250 μM IPTG. To minimize the formation of inclusion bodies, the culture was cooled to 25°C after the addition of IPTG and then further grown for 5 hr at this temperature. Cells were collected by centrifugation and were stored at –70°C. The cell pellet was resuspended in buffer C (20 mM sodium phosphate [pH 7.4], 500 mM NaCl, 100 mM imidazole, 2 mM dithiothreitol, 0.1% CHAPS, 10% (w/v) glycerol) containing Complete protease inhibitor cocktail and sonicated. After centrifugation, the crude cell extract was loaded onto a 1 ml HisTrap HP column equilibrated with buffer C. Then, the column was washed with buffer C containing 300 mM imidazole, and the His-ActVB protein was eluted with 500 mM imidazole in the same buffer. The fractions containing His-ActVB were pooled and dialyzed against a buffer containing 25 mM Tris-HCl (pH 7.5), 0.1% CHAPS, and 10% (w/v) glycerol. Aliquots of the purified protein were stored at –70°C.

Substrates for In Vitro Enzyme Assay

Anthrone and dithranol were purchased from Aldrich and SIGMA, respectively. Anthraquinone (Wako Pure Chemical Industries, Ltd.) and chrysazin (Tokyo Chemical Industry Co., Ltd.) were also purchased for the authenticity of the reaction products. Emodinanthrone **11** was prepared by reduction of emodin **12** (SIGMA) by using excess hydrogen iodide (55% in glacial acetic acid under reflux for 3 hr as previously described (Chen et al., 1995). HR-ESIMS data of the resultant emodinanthrone: m/z [M-H]⁻ 255.0662 (calculated for C₁₅H₁₁O₄, 255.0657). DHK **10** was extracted from liquid culture of *S. tanashiensis* JCM4086 (Johnson and Dietz, 1968) and purified. *S. tanashiensis* was cultured in R5MS medium under the same conditions as those used for *S. coelicolor* in this work. The crude extract obtained with ethyl acetate was purified by silica gel column chromatography eluting chloroform/ethyl acetate/acetic acid (80:20:1) and preparative HPLC by using a Waters Multisolute System under the following conditions: column, TSK gel ODS-100S (7.8 id × 300 mm, TOSO); column temperature, 40°C; solvent, 45% aq. CH₃CN containing 0.5% acetic acid (isocratic); flow rate, 2.0 ml/min.

In Vitro Enzyme Assay

Quinone-forming activity was measured spectrophotometrically by following the increase of absorbance at 490 nm resulting from the formation of emodin from emodinanthrone at 25°C (Chen et al., 1995). Conversion of emodinanthrone to emodin also occurs nonenzymatically, especially under alkaline conditions. Under our assay conditions (pH 7.0), however, the contribution of the nonenzymatic conversion was slight and always less than 10% of that of the enzymatic conversion. The assay mixture (500 μl) for the ActVA-ORF5/ActVB system contained 500 μM NADH, 5 μM FMN, 30% (v/v) ethylene glycol monomethyl ether, 120 U/ml catalase, 100 nM His-ActVB, 1 μM His-ActVA-ORF5, and various amounts of emodinanthrone in 25 mM PIPES-NaOH (pH 7.0). Emodinanthrone in ethyleneglycol monomethylether was subjected to an assay. The assay mixture (500 μl) for ActVA-ORF6 contained 2 μM ActVA-ORF6-His, 30% (v/v) ethyleneglycol monomethylether, and various amounts of the substrate in 25 mM PIPES-NaOH (pH 7.0). The enzymatic conversion of emodinanthrone to emodin was also confirmed by LC/ESIMS analysis. A typical analytical sample was prepared from the foregoing assay mixture as follows. The mixture was extracted with ethyl acetate (500 μl) followed by evaporation to dryness. The residue was dissolved in acetone (100 μl), and an aliquot of the solution (5 μl) was subjected to LC/ESIMS analysis. LC/ESIMS analysis was carried out on a Waters AllianceHT equipped with a photo-diode array detector (Waters 2995) under the following conditions: column, TSK gel ODS-100S (4.6 id × 150 mm, TOSO); column temperature, 40°C; solvent, 45% aq. CH₃CN containing 0.5% acetic acid (isocratic); flow rate, 1.0 ml/min; detection, absorbance between 250 and 600 nm. Mass spectrometry data were obtained under electrospray ionization (ESI) on a Waters LCT-Premier.

DHK monooxygenase activity was detected by LC/ESIMS analysis as described above. DHK (50 μM) was reacted with His-ActVA-ORF5 (1 μM) and His-ActVB (100 nM).

SUPPLEMENTAL DATA

Supplemental Data include five figures and one table and can be found with this article online at [http://www.cell.com/chemistry-biology/supplemental/S1074-5521\(09\)00040-4](http://www.cell.com/chemistry-biology/supplemental/S1074-5521(09)00040-4).

ACKNOWLEDGMENTS

We thank Yutaka Ebizuka for valuable discussion and David A. Hopwood for critical reading of the manuscript. Junya Ochiai is acknowledged for his technical assistance. The authors are grateful for funding to the Effective Promotion of Joint Research of Special Coordination Funds (to K.O.), Grant-in-Aid for Young Scientists from the Ministry of Education, Culture, Sports, Science and Technology (MEXT) (18710189 to T.T.), and Grant-in-Aid for Scientific Research from the Japan Society for the Promotion of Science (20510205 to K.I.). A part of this work was financially supported by the "High-Tech Research Center" Project for Private Universities: matching fund subsidy from MEXT, 2004–2008, and the Uehara Memorial Foundation to K.I.

Received: November 19, 2008

Revised: January 22, 2009

Accepted: January 28, 2009

Published: February 26, 2009

REFERENCES

- Bechthold, A., Sohng, J.K., Smith, T.M., Chu, X., and Floss, H.G. (1995). Identification of *Streptomyces violaceoruber* Tü22 genes involved in the biosynthesis of granaticin. *Mol. Gen. Genet.* **248**, 610–620.
- Beltran-Alvarez, P., Cox, R.J., Crosby, J., and Simpson, T.J. (2007). Dissecting the component reactions catalyzed by the actinorhodin minimal polyketide synthase. *Biochemistry* **46**, 14672–14681.
- Bentley, S.D., Chater, K.F., Cerdeño-Tárraga, A.M., Challis, G.L., Thomson, N.R., James, K.D., Harris, D.E., Quail, M.A., Kieser, H., Harper, D., et al. (2002). Complete genome sequence of the model actinomycete *Streptomyces coelicolor* A3(2). *Nature* **417**, 141–147.
- Caballero, J.L., Martinez, F., Malpartida, F., and Hopwood, D.A. (1991). Organisations and functions of the actVA region of the actinorhodin biosynthetic gene cluster of *Streptomyces coelicolor*. *Mol. Gen. Genet.* **230**, 401–412.
- Chater, K.F., and Hopwood, D.A. (1993). *Streptomyces*. In *Bacillus subtilis* and Other Gram-Positive Bacteria: Biochemistry, Physiology, and Molecular Genetics, A.L. Sonenshein, J.A. Hoch, and R. Losick, eds. (Washington, D.C.: American Society for Microbiology), pp. 83–89.
- Chen, Z.-G., Fujii, I., Ebizuka, Y., and Sankawa, U. (1995). Purification and characterization of emodinanthrone oxygenase from *Aspergillus terreus*. *Phytochemistry* **38**, 299–305.
- Chung, J.Y., Harada, S., Fujii, I., Ebizuka, Y., and Sankawa, U. (2002). Expression, purification, and characterization of AknX anthrone oxygenase, which is involved in aklavinone biosynthesis in *Streptomyces galilaeus*. *J. Bacteriol.* **184**, 6115–6122.
- Cole, S.P., Rudd, B.A.M., Hopwood, D.A., Chang, C.-J., and Floss, H.G. (1987). Biosynthesis of the antibiotic actinorhodin. Analysis of blocked mutants of *Streptomyces coelicolor*. *J. Antibiot. (Tokyo)* **40**, 340–347.
- Fernández-Moreno, M.A., Martínez, E., Boto, L., Hopwood, D.A., and Malpartida, F. (1992). Nucleotide sequence and deduced functions of a set of cotranscribed genes of *Streptomyces coelicolor* A3(2) including the polyketide synthase for the antibiotic actinorhodin. *J. Biol. Chem.* **267**, 19278–19290.
- Fernández-Moreno, M.A., Martínez, E., Caballero, J.L., Ichinose, K., Hopwood, D.A., and Malpartida, F. (1994). DNA sequence and functions of the actVI region of the actinorhodin biosynthetic gene cluster of *Streptomyces coelicolor* A3(2). *J. Biol. Chem.* **269**, 24854–24863.
- Florian, B., and Bibb, M. (1996). *afsR* is a pleiotropic but conditionally required regulatory gene for antibiotic production in *Streptomyces coelicolor* A3(2). *Mol. Microbiol.* **21**, 385–396.
- Huang, J., Lih, C.J., Pan, K.H., and Cohen, S.N. (2001). Global analysis of growth phase responsive gene expression and regulation antibiotic biosynthetic pathways in *Streptomyces coelicolor* using DNA microarrays. *Genes Dev.* **15**, 3183–3192.
- Ichinose, K., Bedford, D.J., Tornus, D., Bechthold, A., Bibb, M.J., Reville, W.P., Floss, H.G., and Hopwood, D.A. (1998a). The granaticin biosynthetic gene cluster of *Streptomyces violaceoruber* Tü22: sequence analysis and expression in a heterologous host. *Chem. Biol.* **5**, 647–659.
- Ichinose, K., Taguchi, T., Ebizuka, Y., and Hopwood, D.A. (1998b). Biosynthetic gene clusters of benzoisochromanequinone antibiotics in *Streptomyces* spp. –identification of genes involved in post-PKS tailoring steps–. *Actinomycetologica* **12**, 99–109.
- Ichinose, K., Surti, C., Taguchi, T., Malpartida, F., Booker-Milburn, K.I., Stephenson, G.R., Ebizuka, Y., and Hopwood, D.A. (1999). Proof that the actVI genetic region of *Streptomyces coelicolor* A3(2) is involved in stereospecific pyran ring formation in the biosynthesis of actinorhodin. *Bioorg. Med. Chem. Lett.* **9**, 395–400.
- Ichinose, K., Ozawa, M., Itou, K., Kunieda, K., and Ebizuka, Y. (2003). Cloning, sequencing, and heterologous expression of the medermycin biosynthetic gene cluster of *Streptomyces* sp. AM-7161: towards comparative analysis of the benzoisochromanequinone gene clusters. *Microbiology* **149**, 1633–1645.
- Itoh, T., Taguchi, T., Kimberley, M.R., Booker-Milburn, K.I., Stephenson, G.R., Ebizuka, Y., and Ichinose, K. (2007). Actinorhodin biosynthesis: structural requirements for post-PKS tailoring intermediates revealed by functional analysis of ActVI-ORF1 reductase. *Biochemistry* **46**, 8181–8188.
- Johnson, L.E., and Dietz, A. (1968). Kalafungin, a new antibiotic produced by *Streptomyces tanashiensis* strain Kala. *Appl. Microbiol.* **16**, 1815–1821.
- Kendrew, S.G., Harding, S.E., Hopwood, D.A., and Marsh, E.N.G. (1995). Identification of a flavin:NADH oxidoreductase involved in the biosynthesis of actinorhodin. Purification and characterization of the recombinant enzyme. *J. Biol. Chem.* **270**, 17339–17343.
- Kendrew, S.G., Hopwood, D.A., and Marsh, E.N.G. (1997). Identification of a monooxygenase from *Streptomyces coelicolor* A3(2) involved in biosynthesis of actinorhodin: purification and characterization of the recombinant enzyme. *J. Bacteriol.* **179**, 4305–4310.
- Kieser, T., Bibb, M.J., Buttner, M.J., Chater, K.F., and Hopwood, D.A. (2000). *Practical Streptomyces Genetics* (Norwich, UK: The John Innes Foundation).
- Kim, I.C., and Oriol, P.J. (1995). Characterization of the *Baicillus stearothermophilus* BR219 phenol hydroxylase gene. *Appl. Environ. Microbiol.* **61**, 1252–1256.
- Korman, T.P., Tan, Y.H., Wong, J., Luo, R., and Tsai, S.C. (2008). Inhibition kinetics and emodin cocrystal structure of a type II polyketide ketoreductase. *Biochemistry* **47**, 1837–1847.
- Malpartida, F., and Hopwood, D.A. (1984). Molecular cloning of the whole biosynthetic pathway of a *Streptomyces* antibiotic and its expression in a heterologous host. *Nature* **309**, 462–464.
- McDaniel, R., Ebert-Khosla, S., Hopwood, D.A., and Khosla, C. (1993). Engineered biosynthesis of novel polyketides. *Science* **262**, 1546–1550.
- Munro, A.W., Girvan, H.M., and McLean, K.J. (2007). Variation on a (t)heme – novel mechanisms, redox partners and catalytic functions in the cytochrome P450 superfamily. *Nat. Prod. Rep.* **24**, 585–609.
- Rudd, B.A.M., and Hopwood, D.A. (1979). Genetics of actinorhodin biosynthesis by *Streptomyces coelicolor* A3(2). *J. Gen. Microbiol.* **114**, 35–43.
- Sambrook, J., Fritsch, E.F., and Maniatis, T. (1989). *Molecular Cloning: A Laboratory Manual*, Second Edition (Cold Spring Harbor, NY: Cold Spring Harbor Laboratory).
- Sciara, G., Kendrew, S.G., Miele, A.E., Marsh, N.G., Federici, L., Malatesta, F., Schimperna, G., Sanvino, C., and Vallone, B. (2003). The structure of ActVA-Orf6, a novel type of monooxygenase involved in actinorhodin biosynthesis. *EMBO J.* **22**, 205–215.
- Shen, B., and Hutchinson, C.R. (1993). Tetracenomylin F1 monooxygenase: oxidation of naphthacene to a naphthacenequinone in the biosynthesis of tetracenomylin C in *Streptomyces glaucescens*. *Biochemistry* **32**, 6656–6663.

- Sherman, D.H., Malpartida, F., Bibb, M.J., Kieser, H.M., Bibb, M.J., and Hopwood, D.A. (1989). Structure and deduced function of the granaticin-producing polyketide synthase gene cluster of *Streptomyces violaceoruber* Tü22. *EMBO J.* *8*, 2717–2725.
- Taguchi, T., Itou, K., Ebizuka, Y., Malpartida, F., Hopwood, D.A., Surti, C.M., Booker-Milburn, K.I., Stephenson, G.R., and Ichinose, K. (2000). Chemical characterisation of disruptants of the *Streptomyces coelicolor* A3(2) *actVI* genes involved in actinorhodin biosynthesis. *J. Antibiot. (Tokyo)* *53*, 144–152.
- Taguchi, T., Okamoto, S., Itoh, T., Ebizuka, Y., Ochi, K., and Ichinose, K. (2008). Actinoperylon, a novel perylenequinone-type shunt product, from a deletion mutant of the *actVA*-ORF5 and ORF6 genes for actinorhodin biosynthesis in *Streptomyces coelicolor* A3(2). *Tetrahedron Lett.* *49*, 1208–1211.
- Valton, J., Filisetti, L., Fontecave, M., and Nivière, V. (2004). A two-component flavin-dependent monooxygenase involved in actinorhodin biosynthesis in *Streptomyces coelicolor*. *J. Biol. Chem.* *279*, 44362–44369.
- Valton, J., Fontecave, M., Douki, T., Kendrew, S.G., and Nivière, V. (2006). An aromatic hydroxylation reaction catalyzed by a two-component FMN-dependent monooxygenase. The ActVA-ActVB system from *Streptomyces coelicolor*. *J. Biol. Chem.* *281*, 27–35.
- Valton, J., Mathevon, C., Fontecave, M., Nivière, V., and Ballou, D.P. (2008). Mechanism and regulation of the two-component FMN-dependent monooxygenase ActVA-ActVB from *Streptomyces coelicolor*. *J. Biol. Chem.* *283*, 10287–10296.
- Zhao, B., Lamb, D.C., Lei, L., Kelly, S.L., Yuan, H., Hachey, D.L., and Waterman, M.R. (2007). Different binding modes of two flavin substrate molecules in cytochrome P450 158A1 (CYP158A1) compared to CYP158A2. *Biochemistry* *46*, 8725–8733.